3-TMA PROXYL: A high-potential, highly soluble nitroxide for enhanced stability and performance in aqueous organic redox flow batteries

Karime Boutamine, Patricia Bassil, Sébastien Gauden, Gilles Casano, Frederic Favier, Olivier Ouari, Steven Le Vot

Energy Storage Materials 80 (2025) 104379

Contents lists available at ScienceDirect

Energy Storage Materials

journal homepage: www.elsevier.com/locate/ensm

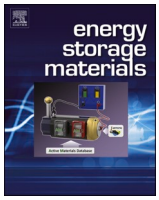

3-TMA PROXYL: A high-potential, highly soluble nitroxide for enhanced stability and performance in aqueous organic redox flow batteries

Karime Boutamine [a,b,c], Patricia Bassil [b,c], Sébastien Gauden [a,c], Gilles Casano [a,c], Frederic Favier [b,c], Olivier Ouari [a,c,*], Steven Le Vot [b,c,*]

[a] Aix-Marseille University, CNRS, ICR UMR7273, Marseille, France
[b] ICGM, University Montpellier, CNRS, ENSCM, Montpellier 34095, France
[c] Réseau sur le Stockage Électrochimique de l'Énergie (RS2E), CNRS, Amiens 80000, France

ARTICLE INFO

Keywords:
3-TMA PROXYL
Nitroxides
Aqueous organic redox flow battery (AORFB)
High redox potential posolytes
Solubility and stability posolytes

ABSTRACT

In response to the growing demand for sustainable and efficient stationary energy storage solutions, this study introduces and evaluates a novel posolyte, 3-TMA PROXYL, tailored for aqueous organic redox flow battery (AORFB) applications. Easily synthesized at the gram scale, 3-TMA PROXYL presents an unprecedented combination of high redox potential (1.06 V vs SHE) and remarkable solubility (> 3 M in 1 M NaCl), resulting in an increased theoretical capacity of 80 Ah L^{-1}. Paired with methyl viologen as a negolyte, the 3-TMA PROXYL battery achieves an 8 % improvement in cell voltage (1.45 V) surpassing the benchmark 4-TMA TEMPO in energy and power density and competing with it regarding stability. Detailed ^{1}H NMR and UV–visible spectroscopy analyses indicate that 3-TMA PROXYL undergoes minimal irreversible chemical degradation, with observed capacity fade attributed primarily to self-discharge. These results establish 3-TMA PROXYL as a reliable alternative to state-of-the-art nitroxides, paving the way for five-membered ring nitroxides in high-performance, sustainable redox flow applications.

1. Introduction

To drastically decrease fossil fuel consumption, it is expected that renewable energies will take up more and more space in the global energy mix. In this context, flexible capacity will be indispensable and will come from grid management itself (automatic limitation, curtailment) but also from indirect levers such as electrochemical storage or power-to-gas conversion. Nowadays, it is widely accepted that battery storage is a mature solution and as such the easiest and the most efficient one. In this context, the stationary energy storage market is growing at a very high pace. Indeed, the international energy agency estimate that for the world electricity sector, battery storage will count for 5 % (1500 GW) in 2030 and >10 % in 2025 (3000 GW) [1].

Currently, lead-acid batteries and lithium-ion batteries (LIB) occupy the principal market of energy storage. For obvious reasons, the lead-acid battery is not suitable for mass energy storage. LIB, driven by the development of the electric vehicle, is the reference technology with energy density superior to 300 Wh kg^{-1} and cost almost below 100€ kWh^{-1}. However, main bottlenecks are the safety issue due to the use of organic electrolyte and Li availability and environmental impact. R&D community thus faces the following scientific challenge: to develop batteries for stationary energy storage that combines sufficient energy, high power and heavy use, going through multiple deep cycles per day, with a long lifetime and maximum safety, while including optimal sustainability in the entire supply chain (substitution of CRM, second-life, and recycling…). It appears that aqueous secondary batteries based on economical and safe materials, and environmentally friendly electrolytes with high ionic conductivity, are critical to revolutionize the battery market.

Redox flow batteries (RFB) are composed of large external tanks containing solubilized redox species and a stack of electrochemical cells in which redox reactions occurs with the electrolyte flowing through carbon felts electrodes [2,3]. RFB are actually a large family of electrochemical devices that have been studied using many chemical configurations (nature of redox species, nature of the solvents, etc.). As a key advantage over other technologies, RFB decouple power and

* Corresponding authors at: Institut Charles Gerhardt Montpellier - UMR 5352, Campus CNRS - Bâtiment Balard – N2F14, 1919, Route de Mende, 34 293 Montpellier Cedex 5), France.
E-mail addresses: olivier.ouari@univ-amu.fr (O. Ouari), steven.le-vot@umontpellier.fr (S.L. Vot).

https://doi.org/10.1016/j.ensm.2025.104379
Received 14 February 2025; Received in revised form 16 May 2025; Accepted 6 June 2025
Available online 8 June 2025

capacity, offering safety high flexibility for large-scale energy storage [4,5]. Vanadium RFB (VRFB) is one of the most commercialized long-term battery technologies but suffers from several major drawbacks including electrolyte imbalance, contamination and cell components corrosion that cause issues regarding long term stability of the system. Nowadays, existing VRFB are in the range of 300 – 800 US$·kWh^{-1} [6,7]. The low solubility (≈ 2 M) of redox moieties combined to the narrow cell voltage (1.2 V) leads to low energy density (< 50 Wh·L^{-1}). A further detrimental limitation that is the high and volatile cost of vanadium combined to the fact that this element is listed as a critical raw material by European Union (EU), make likely that VRFB may never be a major part of the energy mix.

In the recent year, there has been a renaissance in the interest of organic redox molecules for energy storage applications. This interest has been fueled by their lower cost, scalability, recyclability, and minimal environmental footprint. Since mid-2010′s, many efforts have been devoted to the development of the so-called aqueous organic redox flow battery (AORFB) [8–12]. One of the attractiveness of using organic molecules is the possibility to perform molecular engineering to tune redox active species properties (solubility, redox potential, stability…). An impressive list of organic compounds has been reported but candidates for an industrial development seems to be scarce. We can summarize the advances of a decade of research as follow: Firstly, the batteries that operate at very high pH (13-14) use quinones for the negative compartment (negolyte also named anolyte), and iron coordination complexes ($Fe(CN)_6^{4-}$), which is not an organic molecule, for the positive compartment (posolyte also sometimes named catholyte). Secondly, the batteries that operate at close-to-neutral pH use viologen derivatives for the negolyte and nitroxide radicals (or iron coordination complexes (ferrocene derivatives) for the posolyte.

It appears clearly that redox active species are a key feature for the future development of RFB. Beside the manufacturing cost and pure performance (energy, power), lifetime is a key indicator for the development of RFB.

Nitroxides are stable 6-ring cyclic radicals with advantageous redox potential, kinetics, and chemical stability. The redox reaction is the conversion between nitroxide and its corresponding N-oxoammonium cation. Unfortunately, this latter possesses poor stability due to nucleophilic attack by water and available anions of the electrolyte [13,14]. For nitroxide radicals, many degradation mechanisms are envisaged but they are not clearly identified and quantified. It is more likely that the oxo-ammonium form is the most sensitive and prone to degradation. For instance, oxidized 4-TMA-TEMPO can suffer Hoffman-like elimination, ring opening or elimination of chloromethane (NaCl supporting salt) [14,15]. To overpass stability issue, researches focus on the influence of the linker (R in fourth position), on protecting the cation with bulky moieties and on study the influence of the counter ion [15].

Curiously, the tailoring of nitroxide family has been quite limited, and the large majority of RFB studies involve commercially or readily available TEMPO-derivatives (4-hydroxy-TEMPO, 4-methoxy-TEMPO, 4-N-acetamido-TEMPO derivatives), the state-of-the-art, compound being the 4-TMA TEMPO proposed by the group of Schubert in 2016 (still the best nitroxide up to now) [16].

Nitronylnitroxides are 5-rings nitroxides that are very attractive thanks to their higher redox potential compare to TEMPO derivatives (6-rings). Very recently, Hu et al. reported their utilization as posolyte for aqueous redox flow batteries. 3-carbamoyl-2,2,5,5-tetramethylpyrroline1-oxyl radical exhibits a potential of 0.96 V (SHE) [17]. This study is important because it paves the way for the utilization of 5-rings RAM as posolytes. However, stability remains poor (0.54 % per hour, i.e. >6 % day^{-1}). In a second publication, they propose to encapsulate the pyrroline nitroxide in a cyclodextrin preventing thus degradation of the nitroxide which occurs via a ring-opening process [18]. With a 50:50 ratio between nitroxide and host cyclodextrin, fade rate was improved from 5.23 % day^{-1} to 0.2 % day^{-1}.

In the present study, we have synthesized and investigated a new nitronylnitroxide, namely 3-TMA proxyl, for RFB applications. We have demonstrated that this compound shows among the highest potentials ever reported, combined to excellent solubility and stability in a redox flow battery. We have also demonstrated that this molecule is not chemically altered during battery operation and we have proposed that observed fade rate arises from self-discharge more than from degradation such as ring opening.

2. Materials and methods

2.1. Chemicals and physico-chemical characterizations

All solvents and reagents were obtained from Sigma Aldrich or TCI and were used without further purification. Compounds were purified via chromatography on silica gel (Merck silica gel 60, 230–400 mesh).

Nuclear Magnetic Resonance (NMR) spectra were recorded on a Bruker AVL 300 or 400 spectrometer (1H NMR at 300 MHz or 400 MHz, and 13C NMR at 75.5 MHz or 101 MHz) using deuterated solvents. Additional 1H NMR spectra (400 MHz) using an H_2O/D_2O mixture for post-mortem redox flow electrolytes analysis were recorded on a Bruker Avance III HD. Chemical shifts for protons are reported in parts per million (ppm).

Mass spectrometry analyses were conducted using a Q-STAR Elite system, and a Bruker Hybrid Q-TOF system (resolution 7000, mass range 20–8000 Da, mass accuracy < 5 ppm) for post-mortem redox flow electrolytes analysis.

Electron Paramagnetic Resonance (EPR) experiments were carried out using a Bruker Elexsys spectrometer operating at 9.4 GHz (X-band).

2.2. Electrochemical characterizations

All measurements were recorded using a VMP3 Biologic potentiostat. Cyclic voltammetry (CV) and linear sweep voltammetry (LSV) experiments were conducted employing a three-electrode configuration. A rotating glassy carbon electrode (RDE for Rotating Disk Electrode) with a surface area of 0.1963 cm^2 was used as the working electrode, a platinum wire was used as the counter electrode, and an Ag/AgCl electrode immersed in saturated KCl (0.199 V vs. SHE) served as the reference electrode.

2.3. Flow cell cycling method

Redox flow battery tests were conducted using a custom-built cell from Kemiwatt (Rennes, France). The cell was equipped with graphite felt electrodes (SGL Carbon SE, thermally treated) measuring 50 × 50 × 4.65 mm^3, providing a geometric surface area of 25 cm^2. Composite graphite current collectors and an anion-selective membrane, Fumasep FAA-3–50 (thickness 45–55 μm, surface area 25 cm^2) from Fuel Cell Store, Bryan, Texas, USA, were also included in the cell. Electrolyte preparation was as follows: 5 mmol of the nitroxide derivative was dissolved in 50 mL of a 1 M NaCl aqueous solution to prepare the positive electrolyte (posolyte). Similarly, 7.5 mmol of methyl viologen was dissolved in 75 mL of a 1 M NaCl aqueous solution to prepare the negative electrolyte (negolyte). The battery was charged to 100 % state of charge (SOC) at a current density of 10 mA cm^{-2}. Upon reaching the voltage cut-off, a constant potential was maintained until the current density decreased to 1 mA cm^{-2}.

After the batteries were fully charged, 25 mL of the posolyte was removed and stored under the same conditions as the batteries to study the stability of the compounds at 100 % SOC. The batteries were then cycled (10 mA cm^{-2}, 40 ml min^{-1}) for 7 days under an inert atmosphere (glove bag under nitrogen atmosphere).

3. Results and discussion

3.1. Synthesis

From studies previously published by Bo Hu et al., it appears that ring size has an influence on the redox potential of cyclic nitroxides [17]. Additionally, several authors have noted that the trimethylammonium group plays a favorable role in posolyte properties by enhancing the stability of the N-oxoammonium cation [14–16,19–22]. The combination of these two effects represents a promising strategy for developing stable nitroxide/oxoammonium derivatives with higher redox potentials and possible improved performances. Various synthetic strategies were tested, and 3-TMA PROXYL has be synthesized with a 25 % overall yield as described in Scheme 1. It is noteworthy that all the purification steps were performed by precipitation and/or further crystallization, no purification by column chromatography was required.

Compound (1a) was obtained with a yield of 81 % from 2,2,6,6-tetramethylpiperidin-4-one through an alpha-bromination reaction using bromine [23]. Subsequently, compound (1b) was prepared via a Favorskii rearrangement using an aqueous ammonia solution and an excess of potassium hydroxide. The hydrogenation of the double bond using palladium on charcoal as catalyst yielded the carboxamide derivative (1c) with a 99 % yield. Oxidation of the amine of compound (1c) by hydrogen peroxide I, the presence of sodium tungstate produced the nitroxide (1d) with a 62 % yield [24]. Hoffmann rearrangement of the carboxamide group by sodium hypobromite leads to amino-Proxyl (1e) in a 64 % yield [25]. Finally, 3-TMA PROXYL derivative (1) was obtained in 88 % yield by triple N-methylation using iodomethane, followed by an anion metathesis reaction using an anion exchange resin to obtain the corresponding chloride analogue. The overall reaction yield was 25 %. It is worth noting that, the synthetic procedure has not been optimized, as it falls beyond the scope of this study. More details about the synthesis are available in SI.

The electrochemical properties of 3-TMA Proxyl and 4-TMA TEMPO were determined using CV and RDE in 1 M NaCl aqueous electrolytes. CV is a convenient method for easily assessing the reversibility and redox potential of the system. Fig. S1 shows that the 3-TMA Proxyl behave like quasi-reversibility, i.e. ΔEp is almost independent of the scan rate and approximately 70 mV, with |Ipa/Ipc| close to 1, with an apparent standard redox potential (E°_{app}) of 1.06 V. 4-TMA TEMPO, shows a potential of 0.94 V as reported by Schubert et al. (Fig. S2), confirming the expected increase of potential by +120 mV for 3-TMA Proxyl. Also, the solubility of 3-TMA Proxyl has been determined at least 3 M in 1 M NaCl electrolyte for both reduced (uncharged) and oxidized (charged) states.

3.2. Electrochemical characterizations

To further analyze the redox properties of the compounds, extensive investigations were conducted using CV at various scan rates and RDE experiments at various rotation speeds. The apparent electron transfer rate constant (K°_{app}) and diffusion coefficient (D°_{app}) were determined for 3-TMA Proxyl and 4-TMA TEMPO. Results are reported in Table 1. K°_{app} values are 10.1×10^{-3} and 5.6×10^{-3} cm s^{-1}, depending on the method used (CV or RDE, respectively), achieving the targeted order of magnitude. The diffusion coefficients are 3.4×10^{-6} cm^2 s^{-1} either measured by CV or RDE, also meeting the targeted properties. Beyond the quantitative analysis, values of K°_{app} and D for 3-TMA Proxyl are very close to those of state-of-the-art 4-TMA TEMPO, indicating that 3-TMA Proxyl is a suitable candidate as posolyte in a redox flow battery based on these initial electrochemical assessments.

3.3. Battery testings

Nitroxide based redox flow batteries were assembled using methyl viologen (1,1′-bis(methyl)-4,4′-bipyridinium dichloride) as negolyte. Although methyl viologen is not the best because of its toxicity and overall performance, it has been used in this study because of its

Table 1
Electrochemical properties and solubility data of nitroxides derivatives; [(a)]measured using rotating disk electrode experiments; [(b)]measured using CV experiments; [(1)] Angew. Chem. Int. Ed. 2016, 55, 14,427 –14,430 [16].

Compound	Redox potential V vs SHE	(k^0) Electron transfer rate 0.10^{-3} cm s^{-1}	(D) Diffusion constant 0.10^{-6} cm^2 s^{-1}	Solubility in NaCl (aq) = 1 mol L^{-1}
3-TMA PROXYL	1.06	5.6[(a)] 10.1[(b)]	3.4[(a)] 3.4[(b)]	> 3.0
4-TMA TEMPO	0.94	4.4[(a)] 1.1[(b)]	2.8[(a)] 3.3[(b)]	2.3 [(1)]

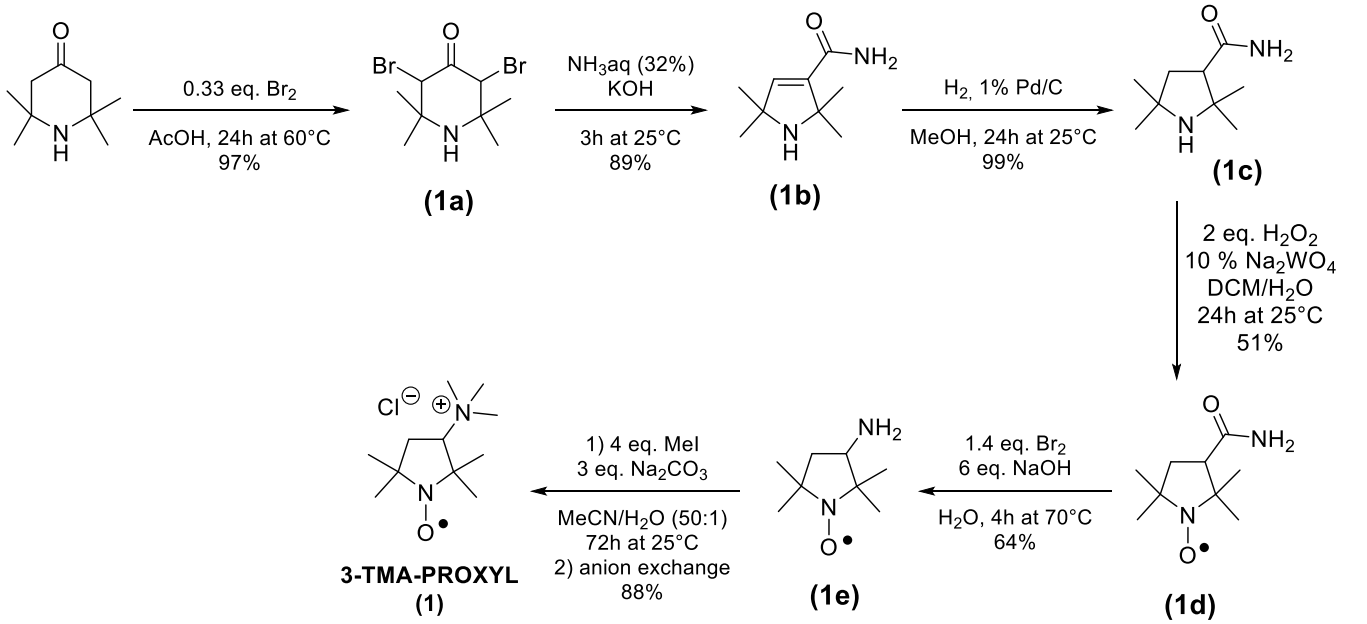

Scheme 1. Synthesis of N,N,N,2,2,5,5-heptamethylpyrrolidinyloxy-3-ammonium chloride (3-TMA PROXYL).

extensive study in the literature as a reference negolyte when evaluating and comparing posolytes. To avoid toxicity issues, sulfonated viologen derivatives [26] or substituted anthraquinones [27–29] could be used but this aspect is beyond the scope of this study. Fig. 1 reports the CVs of redox-active molecules used as negolyte and posolyte. Notably, using 3-TMA Proxyl resulted in a 8 % improvement in cell voltage (1.45 V) compared to 4-TMA TEMPO (1.34 V). Coupled with its excellent solubility, this could lead to further improvements in energy density due to enhanced posolyte capacity. Considering a solubility of 3 M (1 e^- exchanged), the theoretical capacity of the posolyte is 80 Ah L^{-1}, and the energy density of a battery with methyl viologen (2.4 M, 1e^- exchanged) is 52 Wh L^{-1}.

The cycling performance of the prepared redox flow battery is presented in Fig. 2 and compared to the battery using 4-TMA TEMPO as posolyte. Detailed cycling protocols are provided in the experimental section information but it is important to note that, since the posolyte is the focus of this study, the volume of the negolyte was three times larger than that of the posolyte (at the same concentration), resulting in a configuration with a capacity-limiting side (CLS) and a non-capacity-limiting side (NCLS). Improvement in cell voltage (+8 %) is demonstrated in RFB configuration. For 3-TMA PROXYL, the cell voltage is 1.45 V, and the battery exhibits low polarization.

Using galvanostatic cycling (constant current) followed by a potentiostatic regime (constant voltage), a discharge capacity of 55 mAh was obtained, recovering 82 % of the theoretical capacity. As shown in Fig. 3, the capacity then slightly decreases while maintaining excellent coulombic efficiency (> 99 %). For 4-TMA TEMPO, the first discharge led to 62 mAh (Fig. S5), with a subsequent decrease in capacity, although less pronounced than what observed for 3-TMA Proxyl. From Figs. 3 and S5, temporal capacity fade rates of 1.52 % and 1.01 % per day were found for 3-TMA Proxyl and 4-TMA TEMPO, respectively. While 3-TMA Proxyl exhibits a higher fade rate compared to 4-TMA TEMPO, it stands as one of the best capacity fade rates for nitroxide posolytes.

Measuring the power of redox flow batteries at a 50 % state of charge (SOC) provides a robust, predictable, and representative evaluation of performance, facilitating comparisons across various energy storage systems and technologies. At 50 % SOC, which reflects the battery's typical operating charge condition, voltage variations are linear and predictable, simplifying power assessment. Conversely, at very high or very low SOC levels, polarization effects become more pronounced, potentially impacting the accuracy of power measurements. As shown in Fig. S6, the MV/3-TMA PROXYL and MV/4-TMA TEMPO batteries exhibit system resistances of 3.0 Ω·cm² and 3.3 Ω·cm², respectively, in the first cycle, stabilizing around 2.8 Ω·cm² and 2.9 Ω·cm². Interestingly, MV/3-TMA PROXYL and MV/4-TMA TEMPO batteries achieve power densities of 175.7 mW·cm^{-2} and 131.3 mW·cm^{-2}, respectively, in the first cycle, which stabilize at approximately 185.0 mW·cm^{-2} and 147.8 mW·cm^{-2}. Indeed, MV/3-TMA PROXYL battery achieves a power density 25 % higher than MV/4-TMA TEMPO battery, which can be attributed to a similar system resistance but a higher cell voltage.

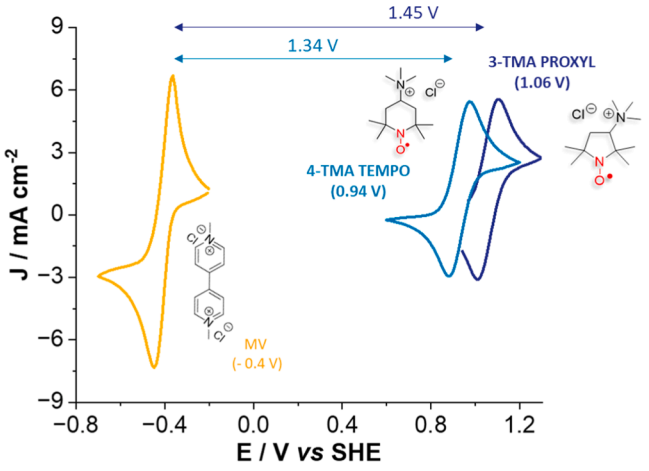

Fig. 1. Cyclic voltammograms of (0.1 M) **3-TMA PROXYL** (dark blue), (0.1 M) **4-TMA TEMPO** (light blue) and (0,1 M) **Methyl viologen** (orange) in (1 M) NaCl (aq) solution.

3.4. Discussion about posolytes caracteritics

The capacity fade rate in redox flow batteries can originate from several issues, mostly crossover of redox-active molecules from one to another tank, and chemical degradation of the redox electrolyte. In aqueous organic redox flow batteries (AORFBs), the latter phenomenon is critical. To identify the origin of capacity losses observed in this study (MV/3-TMA PROXYL and MV/4-TMA TEMPO), CV, UV-visible and ^{1}H NMR spectroscopies, of the posolyte and negolyte solutions were performed, before and after cycling.

Before cycling, CV of the posolyte containing 3-TMA PROXYL (Fig. S7), recorded over an extended potential range, shows the response of the nitroxide/oxoammonium redox couple at 1.06 V. During the negative scan, the reduction of nitroxide into hydroxylamine can be observed in a potential window ranging from −0.4 to −0.7 V. After cycling, two observations can be made. First, the peak current of the nitroxide/ammonium system has decreased, with a current loss (9.7 %) corresponding closely to the battery's capacity loss (10.4 %). Second, oxidized MV is present in the posolyte, indicating that MV passes through the membrane (crossover). Fig. S8 shows that, unlike MV, nitroxides do not cross the membrane from posolyte to negolyte. For 4-TMA TEMPO, similar CVs are observed (Figs. S7 and S8) before and after cycling, as compared to 3-TMA PROXYL. However, the decrease in the exchanged current corresponding to the nitroxide/oxoammonium couple is less pronounced (6.5 %), which also corresponds to the battery's capacity fade (6.9 %).

To eliminate any ambiguity regarding the degradation of 3-TMA PROXYL and 4-TMA TEMPO electrolytes and the possible influence of cycling conditions and/or the presence of methyl viologen, the posolytes at 100 % SOC were stored for the same duration and under identical conditions as those used during battery cycling. These conditions included an inert atmosphere, identical temperature and humidity levels, and strictly controlled storage duration. Based on the cyclic voltammetry results (Fig. S9) after 6.8 days of storage, no significant change (< 2 % variation in Ip) was observed for 3-TMA PROXYL and 4-TMA TEMPO (quasi reversible redox wave at potentials about 0.75 V). The minimal signal losses observed in the CVs fall within the margin of error, indicating little if any degradation of the molecules, as no loss in the concentration of electroactive species was detected.

With freshly charged electrolytes, an irreversible reduction of nitroxide to hydroxylamine [30] is observed at −0.89 V and −0.84 V for 3-TMA PROXYL and 4-TMA TEMPO, respectively. After 6.8 days of storage, the CV profiles changed, as shown in Fig. S9, with a peak at −0.33 V for 3-TMA PROXYL and two peaks at −0.24 V and −0.51 V for 4-TMA TEMPO. Additionally, electrolyte pH changes were observed, with aged electrolytes exhibiting acidic pH levels at 1.44 and 1.41, compared to initial pH values at 5.22 and 4.18 for 3-TMA PROXYL and 4-TMA TEMPO, respectively. Recently, Barbon et al. proposed that oxoammonium ions could react with hydroxide ions, reducing back to nitroxide and producing water and dioxygen, resulting in notable medium acidification [31].

For 4-TMA TEMPO, the peak at −0.51 V is shifted by 0.33 V toward a less negative potential (Fig. S9). Considering that at this pH the reduction mechanism involves a proton-coupled electron transfer with one electron and two protons (resulting in the protonated hydroxylamine form), the observed acidification aligns with the expected 118 mV/pH shift for this electrochemical process. Furthermore, the peak at −0.24 V may be attributed to dissolved oxygen, supporting the hypothesis by

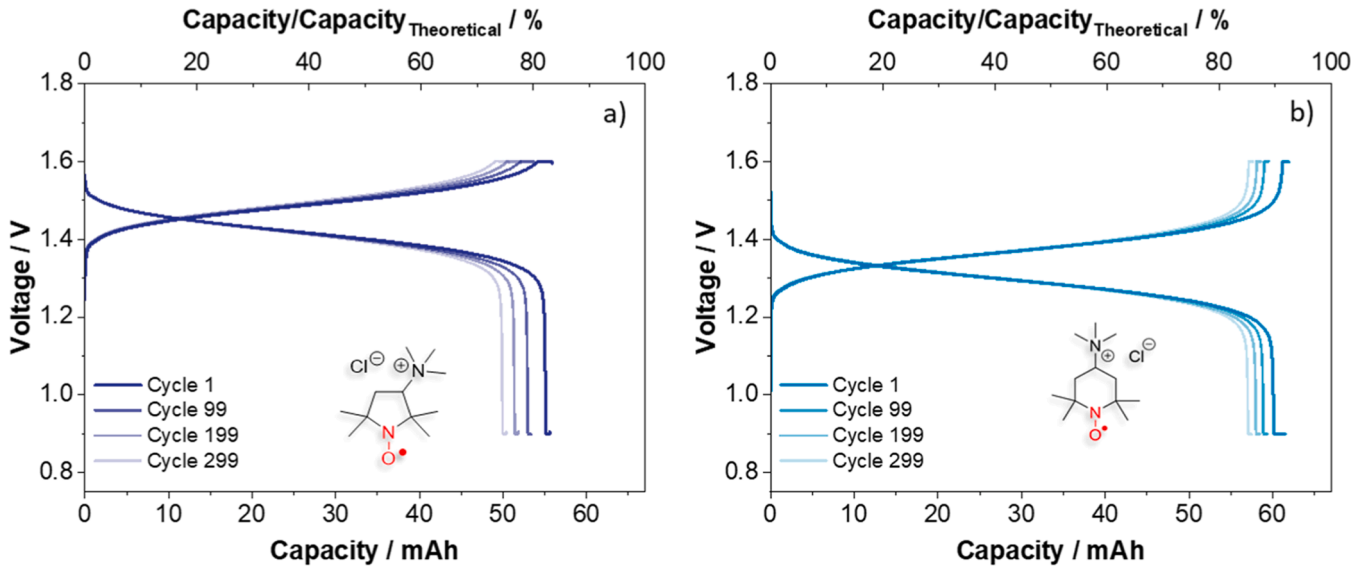

Fig. 2. Voltage vs capacity profiles during cycling for MV/3-TMA PROXYL (a), and MV/4-TMA TEMPO (b) batteries. Negolyte: 75 ml of 0.1 M MV in 1 M NaCl aqueous solution; posolyte: 25 ml of 0.1 M nitroxide in 1 M NaCl; Fumasep FAA-3–50 anion-exchange membrane; SGL Graphite felt (GFD 4.65 EA – 25 cm^2); Current density: 10 $mA{\cdot}cm^{-2}$; Temperature: 23 °C; Flux 40 ml min^{-1}; Duration: 6.8 days.

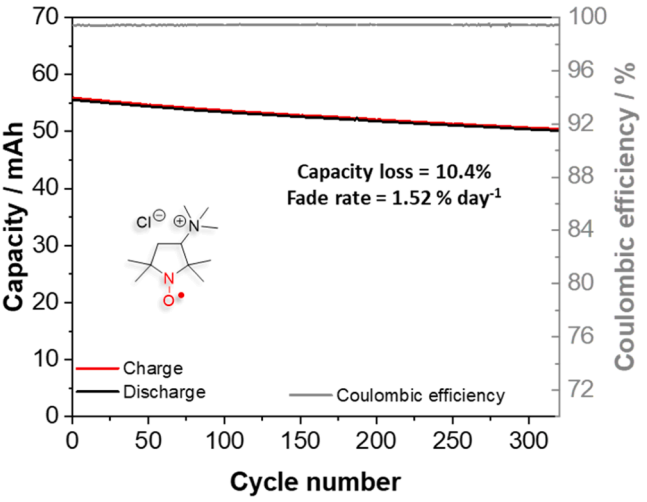

Fig. 3. Charge/discharge capacity vs cycle number profiles for MV/3-TMA PROXYL batteries presented in Fig. 2. Duration: 6.8 days.

Barbon et al. [31]. For 3-TMA PROXYL, a single peak appears at −0.33 V, is more consistent with oxygen reduction. Since the intensity is more pronounced for oxygen reduction in the case of 3-TMA PROXYL, we hypothesize that it may hide the hydroxylamine reduction peak. This observation could also correlate with a faster self-discharge rate, which may explain the slightly lower performance observed in the battery compared to 4-TMA TEMPO.

Based on the UV-visible absorbance spectra of the two posolyte solutions (Figs. 4 and S10), contamination by methyl viologen ($\lambda_{max} = 257$ nm) is observed to induce significant variations in solution absorbance for both posolytes, before and after cycling, thus preventing quantification of nitroxide concentration loss. However, the presence of a band at about 240 nm, corresponding to the nitroxide, with no new chromophore observed, supports the hypothesis that the electrolyte is not irreversibly chemically degraded but rather undergoes self-discharge.

To gain further insights into the degradation products, ^{1}H NMR analyses were performed. Because of the high water content, which risked saturating the NMR signal, the samples were diluted using deuterated water (D_2O). For each sample (0.2 mL), 0.3 mL of D_2O and 3.0 mg of ascorbic acid were added to reduce the paramagnetic nitroxide radicals to hydroxylamines.

Based on the ^{1}H NMR spectra obtained from posolytes before and after cycling, as well as from posolytes stored for 6.8 days at 100 % SOC, several observations were made: The chemical shift of characteristic peaks of 3-TMA PROXYL (Fig. 4), and 4-TMA TEMPO (Fig. S10) differs slightly between the spectra of stored electrolyte and the initial electrolyte. This shift is attributed to a deshielding effect induced by the decreased pH from 5.2 to 1.4 of the stored electrolyte as compared to the initial electrolyte solution. Due to this more acidic pH, the chemical environment of the molecules is altered, resulting in variations in the observed chemical shifts. According to the spectra, this variation is more pronounced for signals (a and b) near the (N—OH) functionality, namely the tetramethyl signals at (1.46; 1.42; 1.30; 1.24 ppm), and (1.32; 1.29 ppm) for 3-TMA PROXYL, and 4-TMA TEMPO, respectively. Very interestingly, for 3-TMA PROXYL, ^{1}H NMR spectra showed no extra peaks after cycling the electrolyte or storage at 100 % SOC compared to the original electrolyte spectrum (Fig. 4), indicating that no irreversible degradation of 3-TMA PROXYL is observed after 6.8 days at 100 % SOC.

For 4-TMA TEMPO, the ^{1}H NMR spectra of the cycled electrolyte showed the appearance of additional, relatively low-intensity peaks in the aliphatic region at 2.17 ppm as a singlet and at 3.20 ppm as a doublet (Fig. S10). The same displacements were detected in the electrolyte stored at 100 % SOC, with a greater intensity than in the cycled electrolyte. This indicates that the degradation of 4-TMA TEMPO originates from its oxidized form. However, given that part of the spectrum between 5.0 and 4.5 ppm is unusable because of signal saturation of water, and the low intensity of degradation product signals hinders accurate integration, it was not possible to deduce a plausible structure for the degradation products from these spectra (4-TMA TEMPO).

TTP-TEMPO [32], 4-OH TEMPO [33–35], CT [17], 4-CO_2Na TEMPO [36], DFTEMPO [37], PSS-TEMPO [38], 4-SO_4Na-TEMPO [39], TMAP-TEMPO [15,21,32], Pyr-TEMPO [40], AcNH-TEMPO [35,41], MiAcNH-TEMPO [41], TMAAcNH-TEMPO [15,22,32], MIMAcO-TEMPO [13,42], Sulfamide-TEMPO [15], CPD [17], 4-NH_2-TEMPO [34,35,43], 4-OT [34], 4-TMA-TEMPO [14–16,32,44,45], N_2-TEMPO [20], N_+-TEMPOD [19], CPL [17], (TPABPy)Cl_3 [46].

4. Conclusion

This work presents the development of 3-TMA PROXYL as a new

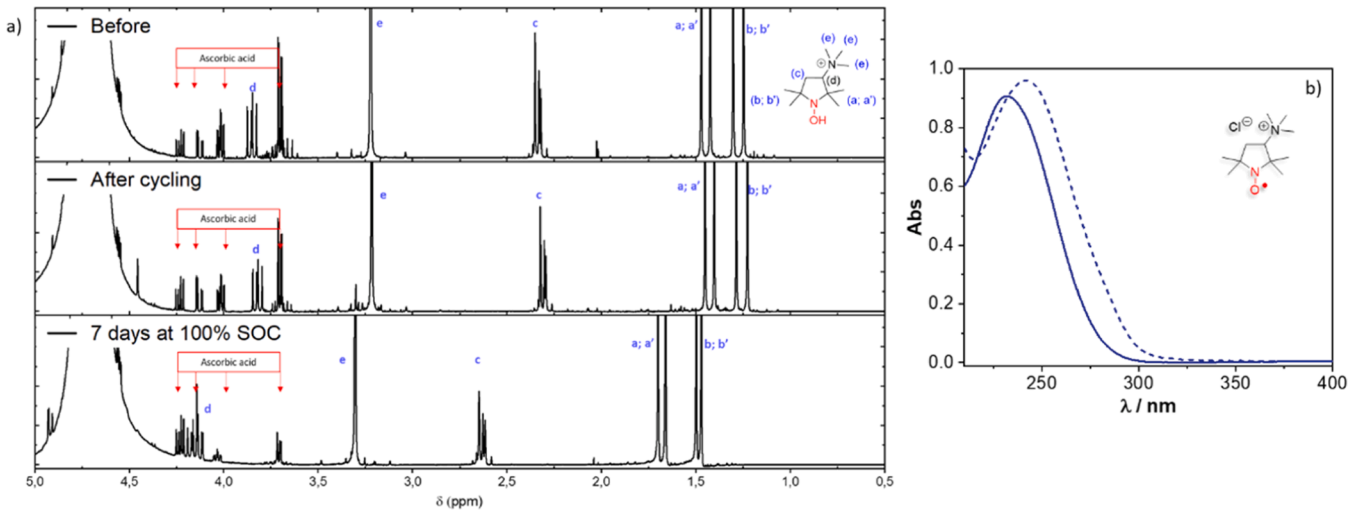

Fig. 4. (a) ^{1}H NMR spectra of the 3-TMA PROXYL electrolyte before and after cycling, and after being stored for 6.8 days in the oxidized state (100 % SOC). (b) UV-visible absorbance spectra of posolytes containing 3-TMA PROXYL before (plain) and after (dashed) cycling.

nitroxide posolyte, that provides the best redox potential and energy density and a scalable and low-cost chemistry. 3-TMA PROXYL has been comprehensively evaluated against the benchmark posolyte 4-TMA TEMPO, demonstrating very good performance. With an 8 % increase in cell voltage, reaching 1.45 V compared to 1.34 V for 4-TMA TEMPO, and exceptional solubility at 3.0 mol L^{-1} in a 1.0 M NaCl solution, 3-TMA PROXYL increases the theoretical posolyte capacity to 80 Ah L^{-1}. Paired with methyl viologen as a negolyte, this novel posolyte yields a record theoretical energy density of 52 Wh L^{-1}. MV/3-TMA PROXYL battery achieves a 25 % greater power density than MV/4-TMA TEMPO battery, and a robust stability profile with minimal signs of irreversible chemical degradation as evidenced by ^{1}H NMR and UV–Visible spectroscopies. While initial capacity losses stabilize after early cycles, 3-TMA PROXYL battery exhibits a daily capacity fade of 1.51 %, compared to 1.01 % for 4-TMA TEMPO.

In summary, 3-TMA PROXYL is distinguished by its high stability, remarkable solubility (>3 M in 1 M NaCl), and one of the highest redox potentials ever reported for AORFB applications (Fig. 5), positioning it as a powerful alternative in redox flow technology. This is the first report of a five-membered ring nitroxide posolyte for AORFBs, offering a compelling balance of high redox potential, solubility and stability, well standing with the state-of-the-art 4-TMA TEMPO. This study thus opens

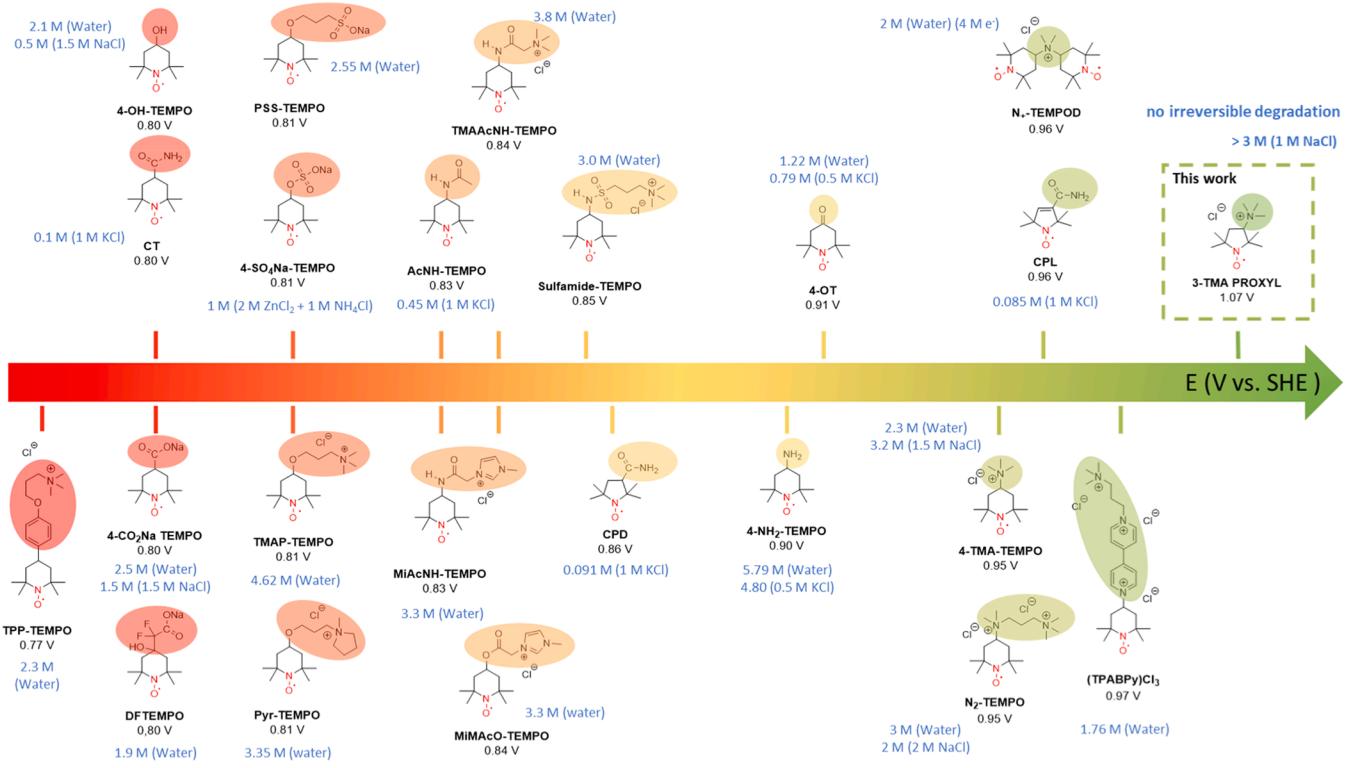

Fig. 5. State-of-the-art positioning of the novel 3-TMA PROXYL nitroxide, highlighting its high solubility and high redox potential, distinguishing it from current benchmark posolytes in AORFB applications. Schematic representation, the potential scale is not respected for clarity purposes. Nitroxides with too poor solubility and/or with no solubility data available have been excluded.

promising avenues for a new class of nitroxide-based posolytes in the development of economical, reliable and long-duration AORFBs.

CRediT authorship contribution statement

Karime Boutamine: Writing – original draft, Methodology, Investigation. **Patricia Bassil:** Writing – original draft, Methodology, Investigation. **Sébastien Gauden:** Methodology, Investigation. **Gilles Casano:** Writing – review & editing, Visualization, Supervision, Formal analysis. **Frederic Favier:** Writing – review & editing, Visualization, Supervision, Formal analysis. **Olivier Ouari:** Writing – review & editing, Validation, Supervision, Project administration, Funding acquisition, Data curation. **Steven Le Vot:** Writing – review & editing, Validation, Supervision, Project administration, Funding acquisition, Data curation.

Declaration of competing interest

The authors declare the following financial interests/personal relationships which may be considered as potential competing interests: Steven Le Vot reports financial support was provided by French National Research Agency. If there are other authors, they declare that they have no known competing financial interests or personal relationships that could have appeared to influence the work reported in this paper.

Acknowledgment

This work was supported by a French government grant from the Agence Nationale de la Recherche (ANR) under the France 2030 program, reference ANR-23-PEBA-0005. ANR is also gratefully acknowledged for funding through the Labex STORE-EX (Grant ANR-10-LABX-76–01)

Supplementary materials

Supplementary material associated with this article can be found, in the online version, at doi:10.1016/j.ensm.2025.104379.

References

[1] International Energy Agency, World Energy Outlook 2023, International Energy Agency, Paris, 2023. https://www.iea.org/reports/world-energy-outlook-2023.
[2] M. Park, J. Ryu, W. Wang, J. Cho, Material design and engineering of next-generation flow-battery technologies, Nat. Rev. Mater. 2 (2016) 16080, https://doi.org/10.1038/natrevmats.2016.80.
[3] A.G. Olabi, M.A. Allam, M.A. Abdelkareem, T.D. Deepa, A.H. Alami, Q. Abbas, A. Alkhalidi, E.T. Sayed, Redox flow batteries: recent development in main components, emerging technologies, diagnostic techniques, large-scale applications, and challenges and barriers, Batteries 9 (2023) 409, https://doi.org/10.3390/batteries9080409. . (Basel).
[4] D. Reber, Electrolyte tank costs are an overlooked factor in flow battery economics, Nat. Energy (2025), https://doi.org/10.1038/s41560-024-01677-6.
[5] D. Reber, S.R. Jarvis, M.P. Marshak, Beyond energy density: flow battery design driven by safety and location, Energy Adv. 2 (2023) 1357–1365, https://doi.org/10.1039/D3YA00208J.
[6] Z. Hou, X. Chen, J. Liu, Z. Huang, Y. Chen, M. Zhou, W. Liu, H. Zhou, Towards a high efficiency and low-cost aqueous redox flow battery: a short review, J. Power. Sources 601 (2024) 234242, https://doi.org/10.1016/j.jpowsour.2024.234242.
[7] K. Amini, A.N. Shocron, M.E. Suss, M.J. Aziz, Pathways to high-power-density redox flow batteries, ACS Energy Lett. 8 (2023) 3526–3535, https://doi.org/10.1021/acsenergylett.3c01043.
[8] J. Winsberg, T. Hagemann, T. Janoschka, M.D. Hager, U.S. Schubert, Redox-Flow-Batterien: von metallbasierten zu organischen aktivmaterialien, Angew. Chem. 129 (2017) 702–729, https://doi.org/10.1002/ange.201604925.
[9] Y. Ding, C. Zhang, L. Zhang, Y. Zhou, G. Yu, Molecular engineering of organic electroactive materials for redox flow batteries, Chem. Soc. Rev. 47 (2018) 69–103, https://doi.org/10.1039/c7cs00569e.
[10] D.G. Kwabi, Y. Ji, M.J. Aziz, Electrolyte lifetime in aqueous organic redox flow batteries: a critical review, Chem. Rev. 120 (2020) 6467–6489, https://doi.org/10.1021/acs.chemrev.9b00599.
[11] P. Fischer, P. Mazúr, J. Krakowiak, Family tree for aqueous organic redox couples for redox flow battery electrolytes: a conceptual review, Molecules 27 (2022) 560, https://doi.org/10.3390/molecules27020560.
[12] F. Zhu, W. Guo, Y. Fu, Functional materials for aqueous redox flow batteries: merits and applications, Chem. Soc. Rev. 52 (2023) 8410–8446, https://doi.org/10.1039/D3CS00703K.
[13] N.-U. Seo, K. Kim, J. Yeo, S.J. Kwak, Y. Kim, H. Kim, M.S. Kim, J. Choi, Y.S. Jung, J. Chae, J. Chang, J.H. Yang, Covalent conjugation of a 'hydroxide-philic' functional group achieving 'hydroxide-phobic' TEMPO with superior stability in all-organic aqueous redox flow batteries, J. Mater. Chem. A (2023), https://doi.org/10.1039/D3TA03420H.
[14] O. Nolte, P. Rohland, N. Ueberschaar, M.D. Hager, U.S. Schubert, Stability of TMA-TEMPO-based aqueous electrolytes for redox-flow batteries, J. Power Sources 525 (2022) 230996, https://doi.org/10.1016/j.jpowsour.2022.230996.
[15] P. Rohland, O. Nolte, K. Schreyer, H. Görls, M.D. Hager, U.S. Schubert, Structural alterations on the TEMPO scaffold and their impact on the performance as active materials for redox flow batteries, Mater. Adv. 3 (2022) 4278–4288, https://doi.org/10.1039/D1MA00663K.
[16] T. Janoschka, N. Martin, M.D. Hager, U.S. Schubert, Wasserbasierte Redox-Flow-Batterie mit hoher kapazität und leistung: das TEMPTMA/MV-System, Angew. Chem. 128 (2016) 14639–14643, https://doi.org/10.1002/ange.201606472.
[17] B. Hu, H. Fan, H. Li, M. Ravivarma, J. Song, Five-membered ring nitroxide radical: a new class of high-potential, stable catholytes for neutral aqueous organic redox flow batteries, Adv. Funct. Mater. 31 (2021) 2102734, https://doi.org/10.1002/adfm.202102734.
[18] H. Fan, K. Liu, X. Zhang, Y. Di, P. Liu, J. Li, B. Hu, H. Li, M. Ravivarma, J. Song, Spatial structure regulation towards armor-clad five-membered pyrroline nitroxides catholyte for long-life aqueous organic redox flow batteries, eScience (2023) 100202, https://doi.org/10.1016/j.esci.2023.100202.
[19] X.-L. Lv, P.T. Sullivan, W. Li, H.-C. Fu, R. Jacobs, C.-J. Chen, D. Morgan, S. Jin, D. Feng, Modular dimerization of organic radicals for stable and dense flow battery catholyte, Nat. Energy 8 (2023) 1109–1118, https://doi.org/10.1038/s41560-023-01320-w.
[20] B. Hu, M. Hu, J. Luo, T.L. Liu, A. Stable, Low permeable TEMPO catholyte for aqueous total organic redox flow batteries, Adv. Energy Mater. 12 (2022), https://doi.org/10.1002/aenm.202102577.
[21] Y. Liu, M.A. Goulet, L. Tong, Y. Liu, Y. Ji, L. Wu, R.G. Gordon, M.J. Aziz, Z. Yang, T. Xu, A long-lifetime all-organic aqueous flow battery utilizing TMAP-TEMPO radical, Chem 5 (2019) 1861–1870, https://doi.org/10.1016/j.chempr.2019.04.021.
[22] H. Fan, W. Wu, M. Ravivarma, H. Li, B. Hu, J. Lei, Y. Feng, X. Sun, J. Song, T.L. Liu, Mitigating ring-opening to develop stable TEMPO catholytes for pH-neutral all-organic redox flow batteries, Adv. Funct. Mater. 32 (2022), https://doi.org/10.1002/adfm.202203032.
[23] G. Sosnovsky, Z. Cai, A study of the Favorskii rearrangement with 3-bromo-4-oxo-2,2,6,6-tetramethylpiperidine-1-oxyl, J. Org. Chem. 60 (1995) 3414–3418, https://doi.org/10.1021/jo00116a029.
[24] C. Sauvée, G. Casano, S. Abel, A. Rockenbauer, D. Akhmetzyanov, H. Karoui, D. Siri, F. Aussenac, W. Maas, R.T. Weber, T. Prisner, M. Rosay, P. Tordo, O. Ouari, Tailoring of polarizing agents in the bTurea series for cross-effect dynamic nuclear polarization in aqueous media, Chem. A Eur. J. 22 (2016) 5598–5606, https://doi.org/10.1002/chem.201504693.
[25] S. Kajigaeshi, T. Nakagawa, S. Fujisaki, A. Nishida, M. Noguchi, Sodium Bromite: a new reagent for the Hofmann degradation of amides, Chem. Lett. 13 (1984) 713–714, https://doi.org/10.1246/cl.1984.713.
[26] S. De La Parra, J.A. Tamayo-Ramos, R. Rubio-Presa, D. Perez-Antolin, V. Ruiz, R. Sanz, C. Rumbo, E. Ventosa, On the tunability of toxicity for viologen-derivatives as anolyte for neutral aqueous organic redox flow batteries, ChemSusChem 16 (2023) e202300626, https://doi.org/10.1002/cssc.202300626.
[27] B. Hu, J. Luo, M. Hu, B. Yuan, T.L. Liu, A pH-neutral, metal-free aqueous organic redox flow battery employing an ammonium anthraquinone anolyte, Angew. Chem. - Int. Ed. 58 (2019) 16629–16636, https://doi.org/10.1002/anie.201907934.
[28] J. Chai, X. Wang, A. Lashgari, C.K. Williams, J. Jiang, A pH-neutral, aqueous redox flow battery with a 3600-cycle lifetime: micellization-enabled high stability and crossover suppression, ChemSusChem 13 (2020) 4069–4077, https://doi.org/10.1002/cssc.202001286.
[29] G. Yang, Y. Zhu, Z. Hao, Q. Zhang, Y. Lu, Z. Yan, J. Chen, An aqueous all-quinone-based redox flow battery employing neutral electrolyte, Adv. Energy Mater. (2024) 2400022, https://doi.org/10.1002/aenm.202400022.
[30] J.B. Gerken, Y.Q. Pang, M.B. Lauber, S.S. Stahl, Structural effects on the pH-dependent redox properties of organic nitroxyls: pourbaix diagrams for TEMPO, ABNO, and three TEMPO analogs, J. Org. Chem. 83 (2018) 7323–7330, https://doi.org/10.1021/acs.joc.7b02547.
[31] A. Barbon, A.A. Isse, A. Gennaro, R. Carmieli, I. Bilkis, L. Weiner, Water oxidation at low potential exploiting a nitroxide/oxoammonium ion redox couple as mediator, Mater. Adv. 3 (2022) 8149–8156, https://doi.org/10.1039/D2MA00668E.
[32] G. Tang, W. Wu, Y. Liu, K. Peng, P. Zuo, Z. Yang, T. Xu, Adjusting Hirshfeld charge of TEMPO catholytes for stable all-organic aqueous redox flow batteries, Nat. Commun. 16 (2025) 47, https://doi.org/10.1038/s41467-024-55244-4.
[33] T. Liu, X. Wei, Z. Nie, V. Sprenkle, W. Wang, A total organic aqueous redox flow battery employing a low cost and sustainable methyl viologen anolyte and 4-HO-TEMPO catholyte, Adv. Energy Mater. 6 (2016), https://doi.org/10.1002/aenm.201501449.
[34] W. Zhou, W. Liu, M. Qin, Z. Chen, J. Xu, J. Cao, J. Li, Fundamental properties of TEMPO-based catholytes for aqueous redox flow batteries: effects of substituent groups and electrolytes on electrochemical properties, solubilities and battery

performance, RSC Adv. 10 (2020) 21839–21844, https://doi.org/10.1039/d0ra03424j.
[35] H. Fan, J. Zhang, M. Ravivarma, H. Li, B. Hu, J. Lei, Y. Feng, S. Xiong, C. He, J. Gong, T. Gao, J. Song, Radical charge population and energy: critical role in redox potential and cycling life of piperidine nitroxyl radical cathodes in aqueous zinc hybrid flow batteries, ACS Appl. Mater. Interfaces 12 (2020) 43568–43575, https://doi.org/10.1021/acsami.0c09941.
[36] B. Liu, C.W. Tang, H. Jiang, G. Jia, T. Zhao, Carboxyl-functionalized Tempo catholyte enabling high-cycling-stability and high-energy-density aqueous organic redox flow batteries, ACS Sustain. Chem. Eng. 9 (2021) 6258–6265, https://doi.org/10.1021/acssuschemeng.0c08946.
[37] L.-C. Yu, Y.-C. Luo, W. Feng, S. Zhang, X. Zhang, Fluorinated TEMPO: a new redox-active catholyte material for aqueous Zn-anode hybrid flow batteries, J. Mater. Chem. A (2023), https://doi.org/10.1039/D3TA02241B.
[38] M. Gao, M. Salla, Y. Song, Q. Wang, High-power near-neutral aqueous all organic redox flow battery enabled with a pair of anionic redox species, Angew. Chem. Int. Ed. 61 (2022) e202208223, https://doi.org/10.1002/anie.202208223.
[39] J. Winsberg, C. Stolze, A. Schwenke, S. Muench, M.D. Hager, U.S. Schubert, Aqueous 2,2,6,6-tetramethylpiperidine-N-oxyl catholytes for a high-capacity and high current density oxygen-insensitive hybrid-flow battery, ACS Energy Lett. 2 (2017) 411–416, https://doi.org/10.1021/acsenergylett.6b00655.
[40] M. Pan, L. Gao, J. Liang, P. Zhang, S. Lu, Y. Lu, J. Ma, Z. Jin, Reversible redox chemistry in pyrrolidinium-based TEMPO radical and extended viologen for high-voltage and long-life aqueous redox flow batteries, Adv. Energy Mater. 12 (2022) 2103478, https://doi.org/10.1002/aenm.202103478.
[41] H. Fan, B. Hu, H. Li, M. Ravivarma, Y. Feng, J. Song, Conjugate-driven electron density delocalization of piperidine nitroxyl radical for stable aqueous zinc hybrid flow batteries, Angew. Chem. Int. Ed. 61 (2022) e202115908, https://doi.org/10.1002/anie.202115908.
[42] Z. Chang, D. Henkensmeier, R. Chen, Shifting redox potential of nitroxyl radical by introducing an imidazolium substituent and its use in aqueous flow batteries, J. Power Sources 418 (2019) 11–16, https://doi.org/10.1016/j.jpowsour.2019.02.028.
[43] J. Cao, F. Ding, H. Chen, H. Wang, W. Wang, Z. Chen, J. Xu, A new redox-active conjugated polymer containing anthraquinone pendants as anode material for aqueous all-organic hybrid-flow battery, J. Power Sources 423 (2019) 316–322, https://doi.org/10.1016/j.jpowsour.2019.03.098.
[44] J. Luo, B. Hu, C. Debruler, T.L. Liu, A π-conjugation extended viologen as a two-electron storage anolyte for total organic aqueous redox flow batteries, Angew. Chem. Int. Ed. 57 (2018) 231–235, https://doi.org/10.1002/anie.201710517.
[45] M. Pan, W. Wang, H. Wang, J. Ma, M. Shao, Z. Jin, High-voltage and durable pH-neutral aqueous redox flow batteries based on quaternary ammonium cations functionalized naphthalene diimide and nitroxyl radical systems, J. Power. Sources 580 (2023) 233269, https://doi.org/10.1016/j.jpowsour.2023.233269.
[46] S. Hu, L. Wang, X. Yuan, Z. Xiang, M. Huang, P. Luo, Y. Liu, Z. Fu, Z. Liang, Viologen-decorated TEMPO for neutral aqueous organic redox flow batteries, Energy Mater. Adv. 2021 (2021) 9795237, https://doi.org/10.34133/2021/9795237, 2021/.